View metadata, citation and similar papers at core.ac.uk
brought to you by CORE
provided by University of Regensburg Publication Server

Resonant tunneling-based spin ratchets

Matthias Scheid[a], Andreas Lassl and Klaus Richter

Institut für Theoretische Physik, Universität Regensburg, 93040 Regensburg, Germany

arXiv:0904.1518v1 [cond-mat.mes-hall] 9 Apr 2009

PACS 72.25.Dc – Spin polarized transport in semiconductors
PACS 73.40.Ei – Rectification
PACS 71.70.Ej – Spin-orbit coupling, Zeeman and Stark splitting, Jahn-Teller effect

Abstract. - We outline a generic ratchet mechanism for creating directed spin-polarized currents in ac-driven double well or double dot structures by employing resonant spin transfer through the system engineered by local external magnetic fields. We show its applicability to semiconductor nanostructures by considering coherent transport through two coupled lateral quantum dots, where the energy levels of the two dots exhibit opposite Zeeman spin splitting. We perform numerical quantum mechanical calculations for the I-V characteristics of this system in the nonlinear regime, which requires a self-consistent treatment of the charge redistribution due to the applied finite bias. We show that this setting enables nonzero averaged net spin currents in the absence of net charge transport.

Introduction. – The field of semiconductor spintronics has seen rapid progress lately, yet there are still many obstacles on the way from fundamental research to operating spin-based devices [1]. The creation of spin polarized currents is one basic requirement for the realization of semiconductor spintronics systems that share the prospect of being able to outperform conventional electronics. Due to a better controlability and faster processing times it is favorable to generate those currents by electrical means, e.g. by the variation of (contact) voltages. Promising classes of devices include spin pumps [2–5], spin rectification [6] and spin ratchets [7–12]. These proposals share the common idea to generate directed spin currents, e.g. mediated by spin-orbit interaction, upon time variation of external potentials. Here we focus on spin ratchets, a generalization of the particle quantum ratchet mechanism [13–15]. In such systems with broken spatial symmetry, pure spin currents are generated by means of an ac-driving with no net average bias. This idea has been put forward for both, nonlinearly driven coherent conductors [7–9], as well as conductors in the dissipative regime, where Brownian particle motion is converted into directed spin currents [10–12]. While a net spin current could be shown to exist for the different settings, its magnitude is difficult to predict and an optimization towards larger spin currents is often not evident.

Here we propose another, generic, spin ratchet mechanism that is based on coherent *resonant* charge and spin transfer. It thereby leads to larger and controllable output and can be implemented in a variety of systems. Moreover, since the ratchet spin currents require operation under nonequilibrium conditions and since the spin currents can usually be enhanced for strong ac-bias, we employ a fully self-consistent treatment of the electrostatics for our quantum transport calculations in the nonequilibrium regime. This involves a self-consistent determination of the voltage drop across the ratchet, which has been approximated so far only by simple heuristic models [7–9].

After outlining the general working principle we focus on a setup invoking resonant tunneling through two quantum dots (QD) in a two-dimensional electron gas (2DEG). In the literature double QD systems have already been proposed as spin filters [16, 17] or sources for pure spin currents [18]. However, these proposals are based on QDs in the Coulomb blockade regime, whereas the double QDs considered here are strong coupled to the leads, i.e. transport is fully coherent and the conductance is larger.

Mechanism. – To illustrate the envisioned spin ratchet mechanism, let us first consider the simplified one-dimensional potential model shown in Fig. 1a). Three electrostatic barriers divide the system into four regions (R1-R4). While the regions R1 and R4 support states with a continuous energy spectrum, the regions R2 and R3, representing the double QD structure, accommodate discrete resonant states due to the confinement imposed

[a] Matthias.Scheid@physik.uni-r.de

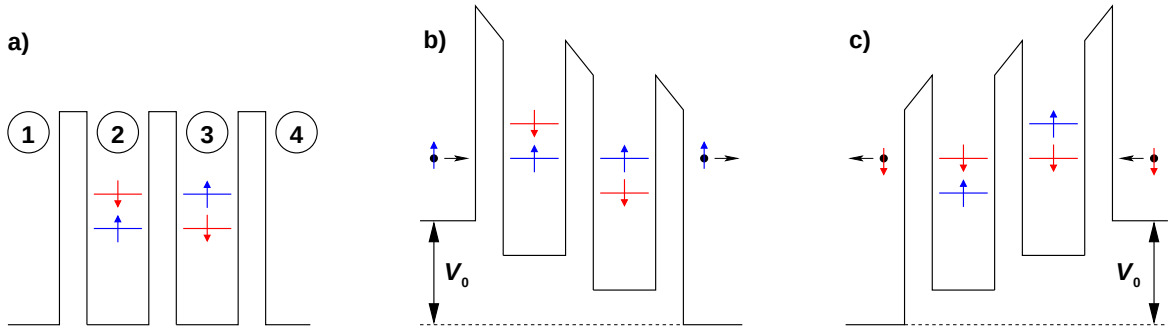

Fig. 1: (*Color online*) Illustration of the working principle of a resonant spin ratchet. Panel a): system devided into four regions R1 to R4 through three barriers. A magnetic field, oriented in opposite directions in regions R2 and R3, splits the levels of spin-up and spin-down electrons (one representative level shown). Panels b,c): Upon application of a positive or negative bias voltage, $\pm V_0$, the transmission probability is resonantly enhanced for spin-up or spin-down electrons, respectively.

by the barriers. We further assume a magnetic field oriented in opposite directions in R2 and R3. Thereby, the resonant energy levels in R2 and R3 are spin split due to the Zeeman coupling, however oppositely in both regions. A finite bias voltage across the device shifts the energy levels in R2 with respect to those in R3. This enables one to bring energy levels of the same spin state in the two QDs into resonance at a specific bias voltage, see Fig. 1b,c). For charge transport through the device, this results in an enhanced transmission of electrons of that specific spin state. Considering both forward and backward bias, it is obvious that the energy levels of different spin states can be brought into resonance for different signs of the bias voltage (see Fig. 1b,c)). Therefore, upon applying an ac-bias to the system, spin can be transported in the absence of a net charge current, as we will confirm below.

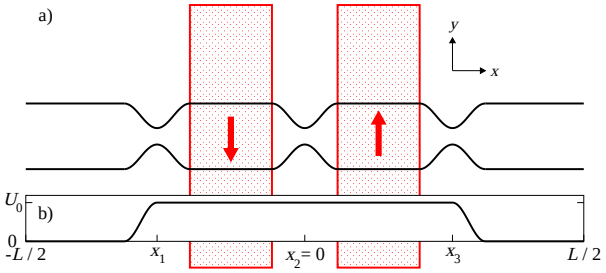

Fig. 2: (*Color online*) a) Possible experimental realization of the principle mechanism for spin current generation described in Fig. 1: Two quantum dots are electrostatically defined (e.g. via side gates) within a quantum wire patterned on a 2DEG. The magnetic fringe fields of two oppositely magnetized ferromagnetic stripes create the opposite Zeeman splitting in the two quantum dots. b) Sketch of an additional electrostatic potential, see text.

System and method. – In Fig. 2 we depict a possible experimental setup, which takes advantage of the principle just described and can be realized with present day material processing techniques. It is based on a quantum wire (QW) patterned on a 2DEG in the (x, y)-plane, see Fig. 2a. Within this wire (in x-direction) which is connected to two non magnetic leads, two QDs possessing discrete energy levels are formed, e.g. via side gates. To realize the opposite Zeeman splitting inside these QDs, two ferromagnetic stripes (FMS) with opposite in-plane magnetization ($\vec{M} = \pm M\hat{y}$) are patterned on top of the semiconductor heterostructure. The fringe fields of the FMS give rise to a non-uniform magnetic field $\vec{B}(x, y)$ in the plane of the 2DEG. We note that the proposed setup is just one possible realization of the mechanism to generate pure spin currents outlined in Fig. 1. Alternatively, one could for instance think of charge transport through resonant tunneling diodes, where the Zeeman splitting can be introduced, e.g., by layers of dilute magnetic semiconductors [19, 20].

The quantum dynamics of electrons in the conductor is described by the single-particle Hamiltonian

$$\mathcal{H} = \frac{\Pi_x^2 + \Pi_y^2}{2m^*} + \frac{g^*\mu_{\rm B}}{2}\vec{B}(x, y)\cdot\vec{\sigma} + V(x, y)\,, \qquad (1)$$

where m^* is the effective mass, g^* the effective gyroscopic factor, $\mu_{\rm B}$ the Bohr magneton, and $\vec{\sigma}$ is the vector of the Pauli spin operators. Orbital effects due to the magnetic field are accounted for by the vector potential $\vec{A}(x, y)$, which enters the momenta $\Pi_i(x, y) = p_i - eA_i(x, y)$, while the Zeeman term $\frac{1}{2}g^*\mu_{\rm B}\vec{B}(x, y)\cdot\vec{\sigma}$ couples the spin degree of freedom to the external magnetic field $\vec{B}(x, y)$ due to the FMS. For this setup $\vec{B}(x, y)$ can be evaluated – along with $\vec{A}(x, y)$ – using standard magnetostatics [21]. The potential $V(x, y)$ includes the lateral confining potential which forms the QW and QDs, a possible potential offset due to an additional gate voltage (see Fig. 2b), as well as the electrostatic potential due to an applied (driving) bias voltage V_0 between the left and right contact to which the QW is connected. The driving is assumed to be adiabatic.

We neglect inelastic processes and assume phase coherent electron transport. The bias $eV_0 = \mu_{\rm L} - \mu_{\rm R}$ induces

an electrical current, which we evaluate in the right lead. Specifically, the current of electrons with spin polarization $\sigma = \pm$ (with respect to a quantization axis in y direction) can be written as

$$I_\sigma(V_0) = \frac{e}{h}\int_{E_C}^{\infty} \mathrm{d}E\, \Delta f(E;V_0) T_\sigma(E;V_0)\,. \qquad (2)$$

Here E_C denotes the energy of the conduction band edge, and $\Delta f(E;V_0) = \left[f(E, E_F + e\frac{V_0}{2}) - f(E, E_F - e\frac{V_0}{2})\right]$ is the difference between the Fermi functions in the two leads. In Eq. (2), the quantum transmission probability for electrons with spin σ is given by

$$T_\sigma(E;V_0) = \sum_{n}^{N_L}\sum_{n'}^{N_R}\sum_{\sigma'=\pm1} |t_{n\sigma,n'\sigma'}(E;V_0)|^2\,, \qquad (3)$$

where $t_{n\sigma,n'\sigma'}$ is the amplitude for transmission from the scattering state $(n'\sigma')$ in the left lead into the scattering state $(n\sigma)$ in the right lead, with the summations running over the $N_{L/R}$ open transversal channels of the left/right lead. These amplitudes are evaluated by projecting the Green's function of the open system onto an appropriate set of asymptotic spinors defining incoming and outgoing channels. Making use of a real-space discretization of the Schrödinger equation [22], the calculation of the $\mathcal{S}$-matrix elements was made feasible by the implementation of a recursive algorithm for the calculation of Green's functions for spin-dependent transport [23].

Self-consistent numerical procedure. – Since ratchet (spin) currents are expected for ac-driving with external bias voltages V_0 in the nonlinear regime, the profile of the electrostatic potential, dropping across the device, may play an important role for the working principle of the ratchet device, and hence its treatment needs special care. In the following we outline our approach to the non-equilibrium quantum transport problem including the self-consistent determination of the electrostatic potential drop arising from the charge rearrangement in the nonlinear bias regime. We consider the classical electrostatic potential $V_{es}(\vec{r})$ described by the Poisson equation, $\vec{\nabla}^2 V_{es}(\vec{r}) = e\rho(\vec{r})/(\varepsilon\varepsilon_0)$, with $\varepsilon = 15.15$ for InAs. The charge density $\rho(\vec{r}) = -e[n(\vec{r}) - n_d(\vec{r})]$ consists of both the density distributions of the electrons, $n(\vec{r})$, and the donors, $n_d(\vec{r})$. The latter is usually not known a priori, while the electron density can be calculated from the lesser Green function $\mathcal{G}^<$, see e.g. [22]:

$$n(\vec{r}) = -\frac{\mathrm{i}}{2\pi}\int \mathrm{d}E\, \mathcal{G}^<(\vec{r},\vec{r};E)\,. \qquad (4)$$

In equilibrium the electrostatic potential is typically included in the effective confinement potential $V = V_{conf} + V_{es}^0$ which we modelled by a hard-wall potential [24]. Therefore, the equilibrium electrostatic potential, governed by $\vec{\nabla}^2 V_{es}^0(\vec{r}) = -e^2\left[n_0(\vec{r}) - n_d(\vec{r})\right]/(\varepsilon\varepsilon_0)$, with $n_0(\vec{r})$ the electron density for zero-bias, need not be considered explicitly. Thus, in the nonequilibrium situation with a finite source-drain bias, only the change of the electrostatic potential $\delta V_{es} = V_{es} - V_{es}^0$ due to the charge rearrangement $\delta n = n - n_0$ of the electrons has to be included, similar as described in Ref. [25]. Hence the Poisson equation

$$\vec{\nabla}^2 \delta V_{es}(\vec{r}) = -\frac{e^2}{\varepsilon\varepsilon_0}\Big[n(\vec{r}) - n_0(\vec{r})\Big]. \qquad (5)$$

has to be solved.

To account for the influence of the leads it is convenient to write the electrostatic potential as a sum, $\delta V_{es} = V_{bias} + V_{el}$ [25]. Here, V_{bias} is the potential induced by the contacts ignoring the charges in the device. It is the solution of the Laplace equation $\vec{\nabla}^2 V_{bias}(\vec{r}) = 0$ with boundary conditions $V_{bias}(x = \pm L/2) = \pm eV_0/2$, where L is the distance between the contacts. For three-dimensional contacts, V_{bias} has the shape of a linear ramp. The contribution of the charges inside the system is described by V_{el}, which is the solution of Eq. (5) with the boundary conditions of $V_{el}(x = \pm L/2) = 0$ at the interfaces of the contacts.

If the electron density in the leads is substantially higher than in the device, the potential drop is screened in the leads leading to a flat electrostatic potential close to the contacts. Then, $n(\vec{r}\,') \approx n_0(\vec{r}\,')$ far from the device, and we can compute the electrostatic potential as

$$V_{el}(\vec{r}) = \frac{e^2}{4\pi\varepsilon\varepsilon_0}\int \mathrm{d}^2 r' \frac{n(\vec{r}\,') - n_0(\vec{r}\,')}{|\vec{r} - \vec{r}\,'|}, \qquad (6)$$

which is the solution of the Poisson equation for a vanishing potential at infinity.

For the self-consistent solution of the transport problem we compute from Eq. (4)the electron density $n(\vec{r})$ for a given electrostatic potential and obtain an improved profile for the electrostatic potential from $n(\vec{r})$. It is known, however, that the straightforward iteration between Eqs. (4) and (6) typically does not converge [26]. Instead we adapted the Newton-Raphson method introduced in Refs. [26, 27] in order to evaluate the electrostatic potential by means of Eq. (6), which significantly improves the convergence behavior of the self-consistent computation scheme. After calculating the self-consistent electrostatic potential for each value of the source-drain voltage we are able to determine the transport properties of the considered ratchet device using Eq. (2).

Numerical results. – In the inset of Fig. 3 we show the transmission $T(E;0)$ in the linear-response regime, $V_0 \to 0$, at zero magnetic field for the device depicted in Fig. 2. The system's geometry parameters (specified in detail below) and energies are chosen such that the leads carry 3 to 4 transversal modes, while the point contacts only allow for (resonant) tunneling. Thus, we find several sharp transmission peaks corresponding to the discrete resonant energy levels of the two QDs. The peaks appear as doublets due to the inter-dot tunnel splitting.

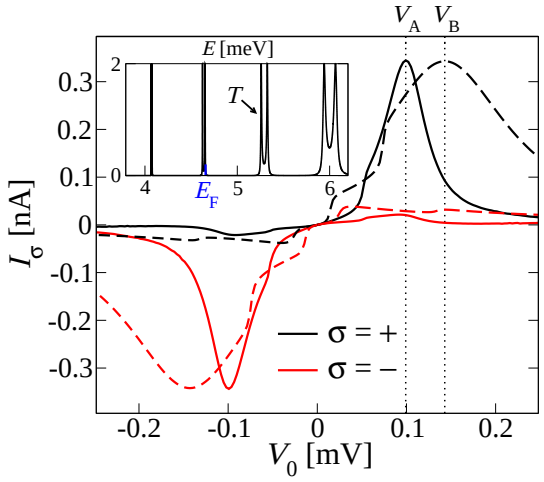

Fig. 3: (*Color online*) Spin resolved currents I_σ for spin-up ($\sigma = +$, black curve) and spin-down ($\sigma = -$, red curve) as a function of applied bias voltage V_0 for an InAs-based double dot device (Fig. 2) at Fermi energy $E_F = 4.66$ meV. The solid (dashed) lines denote the calculation for the self-consistent (model) electrostatic potential drop. Inset: Transmission $T(E, V_0 = 0)$ through the same system at zero magnetic field in linear response.

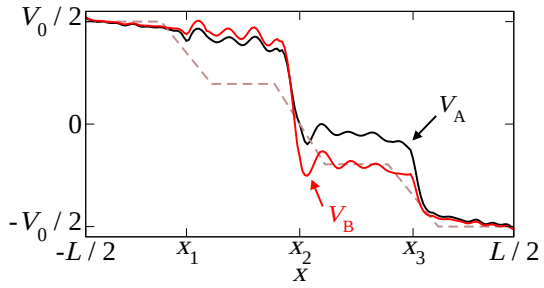

Fig. 4: (*Color online*) Full lines: Self-consistent electrostatic potential drop $V_{es}(x)$ for the two quantum dots bounded by points contacts at $x = x_1, x_2, x_3$ and averaged over the transverse direction. It is shown for bias voltages $V_{A/B}$ as indicated in Fig. 3. The dashed line corresponds to the heuristic voltage drop model (underlying the dashed spin current curves in Fig. 3).

Upon applying a voltage we expect an asymmetric I-V characteristic for the spin resolved currents for Fermi energies close to those resonant energy levels. To conduct explicit calculations for the spin current of the device shown in Fig. 2 we have to fix several parameters. Taking InAs as the material where the 2DEG is built from, we have $m^* = 0.024m_0$ and $g^* = 15$. The width of the QW is chosen to be $W = 200$nm, while at the point contacts, which are separated by 450nm, the width narrows down to 70nm. The two FMS of identical size have dimensions $x_0 = 250$nm, $y_0 = 800$nm, $z_0 = 250$nm and are centered on top of the two point contacts at a distance 50nm above the 2DEG. For the magnetization of the stripes we chose $\mu_0 M = 2.5$T, a value well in reach using e.g. Dysprosium [28]. To allow for a high electron density in the leads in order to screen the electrostatic potential drop and to achieve a flat electrostatic potential in R1 and R4, we include an additional confinement potential $U_0 = 2.92$meV as shown in Fig. 2b).

The spin-resolved I-V characteristics which are obtained with the described procedure for the Fermi energy at the second resonant energy level, $E_F = 4.66$ meV (see inset of Fig. 3), are shown in Fig. 3 as solid lines (black and red line for spin-up and down, respectively). There we find that the device indeed acts as a spin selective current rectifier with dominant ($> 90\%$) spin-up polarization for positive and spin-down polarization for negative bias voltages. This implies that when applying an adiabatically varying unbiased ac-voltage to the contacts the system only transports spins, yet no net charge, since the total charge currents average to zero. The pronounced maximum (minimum) at $\pm V_A$ reflects level alignment, i.e. the resonance condition sketched in Fig. 1. For comparison the dashed lines in Fig. 3 represent the corresponding I_σ-V curves arising from the aforementioned heuristic voltage drop model. It assumes a local voltage drop ($V_0/3$) at each of the three point contacts, i.e. the regions of maximum resistance. We find the same qualitative overall behavior for the spin currents, while the maximum of the resonant tunneling current is reached at a higher value, $V_0 = V_B$ with eV_B being approximately three times the Zeeman splitting of the energy levels of the QD, as expected for this particular model. We performed further calculations (not presented here) which show that the degree of spin polarization, i.e. the efficiency of the device, increases with the Zeeman splitting in regions R2 and R3, due to the stronger separation of the spin $-\sigma$ energy levels at resonance for spin σ. Accordingly, the optimal working condition, i.e. levels for one spin species at resonance, is then reached at higher voltages.

Since the amount of voltage that drops at the central point contact determines the alignment of the energy levels of the two QDs, in Fig. 4 we study the profile of the self-consistent electrostatic potential, $V_{es}(x)$, along the transport direction for applied bias $V_0 = V_A$ (full black line) and V_B (full red line) with $V_{A/B}$ marked in Fig. 3. We see that due to the point contacts a step structure emerges, with its exact form depending on V_0 and E_F. Compared to the heuristic voltage drop model (dashed line), we find a stronger voltage drop at the central point contact. This explains that in Fig. 3 the current maximum is reached at lower bias voltages and the currents are significantly smaller at high bias for the self-consistent current calculation. Still, in view of Figs. 3 and 4, we can conclude that the heuristic voltage drop model constitutes a fair approximation to V_{es} for the system considered.

Summary. – In conclusion we have presented a generic mechanism to produce pure spin currents in nanostructures by applying an ac electrical bias. It is based

on resonant transfer of spin-up and -down electrons in opposite directions and gives rise to pure ratchet type spin currents upon driving. Our results are based on self-consistent Keldysh Greens function transport in order to adequately describe the nonequilibrium condictions under which the system works.

* * *

We acknowledge useful conversations with C. Ertler, M. Wimmer and D. Bercioux. The work was funded by the *Deutsche Forschungsgemeinschaft* within SFB 689. MS acknowledges additional funding from *Studienstiftung des Deutschen Volkes*.

REFERENCES

[1] Awschalom D. D. and Flatté M. E., *Nat. Phys.*, **3** (2007) 153.
[2] Mucciolo E. R., Chamon C. and Marcus C. M., *Phys. Rev. Lett.*, **89** (2002) 146802.
[3] Watson S. K., Potok R. M., Marcus C. M. and Umansky V., *Phys. Rev. Lett.*, **91** (2003) 258301.
[4] Sharma P. and Brouwer P. W., *Phys. Rev. Lett.*, **91** (2003) 166801.
[5] Governale M., Taddei F. and Fazio R., *Phys. Rev. B*, **68** (2003) 155324.
[6] Braunecker B., Feldman D. E. and Li F., *Phys. Rev. B*, **76** (2007) 085119.
[7] Scheid M., Wimmer M., Bercioux D. and Richter K., *Phys. Status Solidi (c)*, **3** (2006) 4235.
[8] Scheid M., Pfund A., Bercioux D. and Richter K., *Phys. Rev. B*, **76** (2007) 195303.
[9] Scheid M., Bercioux D. and Richter K., *New J. Phys.*, **9** (2007) 401.
[10] Smirnov S., Bercioux D., Grifoni M. and Richter K., *Phys. Rev. Lett.*, **100** (2008) 230601.
[11] Smirnov S., Bercioux D., Grifoni M. and Richter K., *Phys. Rev. B*, **78** (2008) 245323.
[12] Smirnov S., Bercioux D., Grifoni M. and Richter K., arXiv:0903.2765v1 (unpublished) (2009).
[13] Reimann P., Grifoni M. and Hänggi P., *Phys. Rev. Lett.*, **79** (1997) 10.
[14] Linke H., Humphrey T. E., Lofgren A., Sushkov A. O., Newbury R., Taylor R. P. and P. Omling, *Science*, **286** (1999) 2314.
[15] Hänggi P. and Marchesoni F., *Rev. Mod. Phys.*, **81** (2009) 387.
[16] Cota E., Aguado R., Creffield C. E. and Platero G., *Nanotechnology*, **14** (2003) 152.
[17] Cota E., Aguado R. and Platero G., *Phys. Rev. Lett.*, **94** (2005) 107202.
[18] Sun Q.-f., Guo H. and Wang J., *Phys. Rev. Lett.*, **90** (2003) 258301.
[19] Slobodskyy A., Gould C., Slobodskyy T., Becker C. R., Schmidt G. and Molenkamp L. W., *Phys. Rev. Lett.*, **90** (2003) 246601.
[20] Ertler C. and Fabian J., *Appl. Phys. Lett.*, **89** (2006) 242101.
[21] Jackson J., *Classical Electrodynamics* (John Wiley & Sons, Inc.) 1999.
[22] Ferry D. K. and Goodnick S. M., *Transport in Nanostructures* (Cambridge University Press) 1997.
[23] Lassl A., Schlagheck P. and Richter K., *Phys. Rev. B*, **75** (2007) 045346.
[24] Laux S. E., Frank D. J. and Stern F., *Surf. Sci.*, **196** (1988) 101.
[25] Xue Y., Datta S. and Ratner M. A., *Chem. Phys.*, **281** (2002) 151.
[26] Trellakis A., Galick A. T., Pacelli A. and Ravaioli U., *J. Appl. Phys.*, **81** (1997) 7880.
[27] Lake R., Klimeck G., Bowen R. C. and Jovanovic D., *J. Appl. Phys.*, **81** (1997) 7845.
[28] Uzur D., Nogaret A., Beere H. E., Ritchie D. A., Marrows C. H. and Hickey B. J., *Phys. Rev. B*, **69** (2004) 241301.